

Valley Edelstein Effect in Monolayer Transition Metal Dichalcogenides

Katsuhisa Taguchi,¹ Yuki Kawaguchi,¹ Yukio Tanaka,¹ and Kam Tuen Law²

¹*Department of Applied Physics, Nagoya University, Nagoya, 464-8603, Japan*

²*Department of Physics, Hong Kong University of Science and Technology, Clear Water Bay, Hong Kong, China*

Monolayer transition metal dichalcogenides (MTMDs) exhibit spin-orbit coupling (SOC) called Ising SOC which polarizes electron spins to opposite out-of-plane directions for electrons in opposite valleys. We predict the emergence of the valley Edelstein Effect (VEE), which is an electric-field-induced spin polarization effect, in the MTMDs. We found an unconventional valley-dependent response in which the spin-polarization is parallel to the applied electric field and the spin-polarization is opposite at opposite valleys due to the Ising SOC. This is in sharp contrast to usual Edelstein effect in which the induced spin-polarization is perpendicular to the applied electric field. We attribute the VEE to the valley Hall effect and Ising SOC. Experimental schemes to detect the VEE are also considered.

Introduction.— Monolayer transition metal dichalcogenides (MTMDs) have attracted much attention recently because of their peculiar electronic and optical properties [1]. Semiconducting MTMDs, MX_2 , are composed of transition metal atoms ($\text{M}=\text{Mo}, \text{W}$) and group-VI dichalcogenide atoms ($\text{X}=\text{S}, \text{Se}, \text{Te}, \text{etc.}$) [2–5]. They have two-dimensional (2D) honeycomb lattice structures, and there is a direct band gap between the valence and conduction bands near the $\pm K$ points [6–10]. The top valence and the bottom conduction band of MTMD are spin-split (~ 0.1 eV and ~ 1 meV, respectively) due to the strong spin-orbit coupling (SOC) of the d -orbitals of transition metal atoms and in-plane mirror-symmetry breaking of the lattice structure [11–15]. In particular, the SOC here works as a valley-dependent Zeeman field, called Ising SOC [16, 17], which polarizes electron spins at opposite valleys to opposite out-of-plane directions. Such a valley-dependent band structure enables us to utilize the valley degrees of freedom of electrons, and hence, MTMDs are potential candidates for valleytronics devices [18–20]. So far, several valley-dependent phenomena, such as valley-selective circularly dichroism [21] and valley-Hall effect [22], have been theoretically studied and experimentally reported. Besides, in gated MTMDs, spintronics systems with nonzero Rashba SOC and Ising SOC have been experimentally studied [16].

In this Letter, we show a new type of valley-dependent response of MTMDs to an electric field via the Edelstein effect [1, 2, 23, 25, 27, 28]. The conventional Edelstein effect is the generation of spin polarization in response to an applied in-plane electric field \mathbf{E} in a 2D system with the Rashba SOC [29–32]. The induced spin polarization is perpendicular to the electric current along \mathbf{E} . With the Ising SOC, the induced spin polarization has both perpendicular and parallel-components with respect to \mathbf{E} and the sign of the parallel component depends on the valley index. We call this the valley Edelstein effect (VEE). The VEE is due to the valley Hall effect which generates valley dependent currents perpendicular to \mathbf{E} [see Fig. 1(a)]. This effect allows us to further control the spin polarization direction of the current by \mathbf{E} and

have potential applications in spintronic devices.

To consider the Edelstein effect in a MTMD such as in MoS_2 and WS_2 which are insulating intrinsically, we consider a gated MTMD, as shown in Fig. 1 (b), to tune the chemical potential to the conduction band as performed experimentally [16]. Beside changing the chemical potential of the MTMD, gating also breaks out-of-plane mirror symmetry and induces Rashba SOC [16, 33]. This allows us to investigate the combined effect of the Ising and Rashba SOC on the Edelstein effects. By calculating the induced spin density using Keldysh-Green’s function techniques, we find that the valley-dependent Zeeman field of the Ising SOC triggers the electric-field induced spin density, which is parallel to the applied in-plane elec-

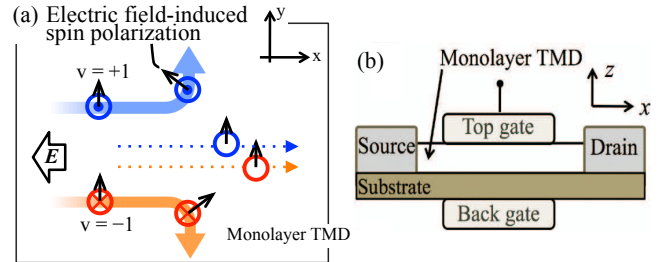


FIG. 1. Schematic of the VEE. The blue and orange arrows represent the motion of electrons in the $v = +1$ and -1 valleys, respectively, induced by an electric field \mathbf{E} applied in the $-x$ direction. The thick solid (thin dotted) arrows correspond to the trajectories in the presence (absence) of the Ising SOC. Due to the valley Hall effect through the Ising SOC, the trajectory of electrons in the $v = +1$ (-1) valley bends into the $+y$ ($-y$) direction. The spin polarization (black arrows) arises in the perpendicular direction to the electron motion via the spin-momentum locking due to the Rashba SOC. As a result, in the presence of the Ising SOC, the valley-dependent spin polarization is induced along \mathbf{E} (VEE) in addition to the net spin polarization perpendicular to \mathbf{E} (conventional Edelstein effect). (b) Setup for the MTMD with tunable chemical potential and Rashba SOC. The former and latter are caused by gating of the gate voltage and by breaking inversion symmetry via the spatial gradient of the voltage along the out-of-plane direction, respectively.

tric field \mathbf{E} and depends on the valley. Specifically, the spin density induced in response to \mathbf{E} is given by

$$\langle \mathbf{s}_v^{\text{VEE}} \rangle = e\nu_e [\mathcal{C}_\perp (\hat{\mathbf{z}} \times \mathbf{E}) + v\mathcal{C}_\parallel \mathbf{E}], \quad (1)$$

where $v = \pm$ is the index denoting the valley degrees of freedom, $e < 0$ is the elementary charge of an electron, $\nu_e = m/(2\pi\hbar^2)$ is the 2D density of states with m being the effective electron mass, $\hat{\mathbf{z}}$ is a unit vector normal to the system, and \mathcal{C}_\perp and \mathcal{C}_\parallel are the response coefficients that we calculate in the following sections. The second term in Eq. (1) is the main result in this work. Because of the valley dependence of the Ising SOC, the direction of the parallel spin component is opposite for opposite valleys. Importantly, in a certain parameter regime, the valley-dependent effect is comparable with the conventional Edelstein effect. We further show that VEE can be detected by using optical Faraday effect [29] and photoluminescence [30, 34] via the valley-selective optical transitions [21].

Model.— We consider a MTMD, such as MoS₂ and WS₂, and assume that the Fermi level crosses the spin-split conduction bands around the $\pm K$ points [4, 6], as shown in Fig. 2. Such situation can be achieved by heavily gating [35, 36]. The effective Hamiltonian $\mathcal{H}_{0,v}$ for electrons in the vK valley is given by [4, 11]

$$\mathcal{H}_{0,v} = \sum_{\mathbf{k}} \psi_v^\dagger [\varepsilon_{\mathbf{k}} + v\beta_I \sigma^z + \alpha_R (k_y \sigma^x - k_x \sigma^y)] \psi_v, \quad (2)$$

where $\psi_v^\dagger \equiv \psi_v^\dagger(\mathbf{k}) = (\psi_{\uparrow,v}^\dagger, \psi_{\downarrow,v}^\dagger)$ is the creation operator of an electron in the valley vK with \uparrow and \downarrow denoting the spin, $\mathbf{k} \equiv (k_x, k_y)$ is the electron momentum measured from the vK point, and σ^i ($i = x, y, z$) are the Pauli matrices. The first term of Eq. (2) is the kinetic term with $\varepsilon_{\mathbf{k}} = \hbar^2 k^2/(2m) - \mu$, where the chemical potential μ is measured from the averaged energy of the spin-split conduction bands at the vK point. The second term is the Ising SOC. The coupling strength β_I is assumed to be a constant [16, 37], since the spin splitting is independent of \mathbf{k} up to the second order near the $\pm K$ points [11–15, 20]. The third term of Eq. (2) is the Rashba SOC whose strength α_R can be controlled by the gate voltage. Without loss of generality, we choose both β_I and α_R to be positive.

We further take into account an in-plane dc electric field \mathbf{E} as well as nonmagnetic impurities on the MTMD. Here, we assume that hybridization between the $\pm K$ valleys can be ignored, namely, the magnitude of the momentum-shift due to \mathbf{E} is much smaller than $2|K|$. Then the Hamiltonian for electrons in the $\pm K$ valleys are decoupled, each of which is given by

$$\mathcal{H}_v = \mathcal{H}_{0,v} + \mathcal{H}_{\text{em},v} + \mathcal{V}_{\text{imp},v}, \quad (3)$$

$$\mathcal{H}_{\text{em},v} = -e \sum_{\mathbf{k}} \psi_v^\dagger \mathbf{v} \cdot \mathbf{A} \psi_v, \quad (4)$$

$$\mathcal{V}_{\text{imp},v} = \int d\mathbf{x} u_i(\mathbf{x}) \psi_v^\dagger(\mathbf{x}) \psi_v(\mathbf{x}), \quad (5)$$

where $\mathbf{v} = -(\partial\mathcal{H}_v/\partial\mathbf{k})/\hbar$ is the velocity operator, \mathbf{A} is the vector potential defined by $\mathbf{E} = -\partial_t \mathbf{A}$, and $u_i(\mathbf{x}) = \sum_{j=1}^{N_i} u_0 \delta(\mathbf{x} - \mathbf{R}_j)$ is the short-range impurity potential independent of the valley index. Here, N_i , u_0 , and \mathbf{R}_j are the number of impurities, a constant impurity potential, and the position of the j th impurity on the monolayer, respectively.

Valley-Edelstein effect.— We calculate the induced spin density using the Keldysh Green's functions within the linear response to \mathbf{E} . The contributions from the $\pm K$ valleys, $\langle \mathbf{s}_\pm^{\text{VEE}} \rangle$, are independently calculated from \mathcal{H}_\pm . We assume that the self-energy Σ_v due to impurity scatterings satisfies $\Sigma_v \ll |\mu \pm \beta_I|$, which allows us to take into account disorder effects perturbatively [1]. For the parameters we choose below, this assumption is satisfied. Using the Keldysh techniques, the spin density in response to \mathbf{E} is found to be [38]

$$\langle \mathbf{s}_v^{\text{VEE},i} \rangle = -\frac{e\hbar}{4\pi} \sum_{\mathbf{k},\omega} \sum_{j=x,y} \frac{df_\omega}{d\omega} \text{tr}[\sigma^i G_{\mathbf{k},\omega,v}^r \mathcal{S}_{\mathbf{k},\omega,v}^j G_{\mathbf{k},\omega,v}^a] E_j, \quad (6)$$

where $G_{\mathbf{k},\omega,v}^r = [\hbar\omega - \mathcal{H}_{0,v} + i\Sigma_v]^{-1}$ and $G_{\mathbf{k},\omega,v}^a = [G_{\mathbf{k},\omega,v}^r]^\dagger$ are the retarded and advanced Green's functions, respectively, f_ω is the Fermi distribution function, and $\mathcal{S}_{\mathbf{k},\omega,v}^j$ is the velocity operator with the ladder vertex corrections. The self-energy Σ_v is calculated within the self-consistent Born approximation, resulting in [38]

$$\Sigma_v = \Sigma'_{0,\omega} + v\Sigma_{z,\omega}\sigma^z, \quad (7)$$

where $\Sigma'_{0,\omega} = \Sigma_0 \equiv \pi n_c u_0^2 \nu_e$ and $\Sigma_{z,\omega} = 0$ for $\mu > \beta_I$ and $\Sigma'_{0,\omega} \equiv \Sigma_0(1 + u_R/\sqrt{\lambda_\omega})/2$ and $\Sigma_{z,\omega} \equiv \Sigma_0 \beta_I/(2\sqrt{\lambda_\omega})$ for $-\beta_I < \mu < \beta_I$. Here, we define $\Sigma_0 = \pi n_c u_0^2 \nu_e$ and $\lambda_\omega = \beta_I^2 - (\mu + \hbar\omega)^2 + [u_R - (\mu + \hbar\omega)]^2$, where n_c is the concentration of impurities and $u_R \equiv m\alpha_R^2/\hbar^2$ is the Rashba energy.

Using the obtained self-energy, the Green's function can be decomposed as

$$G_{\mathbf{k},\omega,v}^r = \frac{\Omega_+^r}{\hbar\omega - E_+ + i(\Sigma'_{0,\omega} + \gamma\Sigma_{z,\omega})} + \frac{\Omega_-^r}{\hbar\omega - E_- + i(\Sigma'_{0,\omega} - \gamma\Sigma_{z,\omega})}, \quad (8)$$

where $E_\pm = \varepsilon_{\mathbf{k}} \pm \sqrt{\alpha_R^2 k^2 + \beta_I^2}$ is the energy dispersion of each band, and $\Omega_\pm^r = 1/2 \pm (\mathbf{u}^r \cdot \boldsymbol{\sigma})/2(\sqrt{\alpha_R^2 k^2 + \beta_I^2} - i\gamma\Sigma_{z,\omega})$ is the projection operator onto the each band with $\mathbf{u}^r = \alpha_R(\mathbf{k} \times \hat{\mathbf{z}}) + v(\beta_I - i\Sigma_z)\hat{\mathbf{z}}$ and $\gamma = \beta_I/\sqrt{\beta_I^2 + \alpha_R^2 k^2}$. It is noticed that the first (second) term of Eq. (8) is the Green's function corresponding to the spin-split upper (lower) conduction band.

After some calculations [39], we find that the magnitude of \mathcal{C}_\perp is comparable to that of \mathcal{C}_\parallel in Eq. (1) when $\mu \gg \beta_I$. Below, we discuss in detail in this parameter

regime. The results for $\mu < \beta_I$ will be given in the Supplementary [39]. For $\mu \gg \beta_I$, we obtain

$$\mathcal{C}_\perp = \frac{\alpha_R}{4\pi} \Gamma^{(v)} \frac{1 - \Gamma_{xx}^{(s)}}{[1 - \Gamma_{xx}^{(s)}]^2 + [\Gamma_{xy}^{(s)}]^2}, \quad (9)$$

$$\mathcal{C}_\parallel = \frac{\alpha_R}{4\pi} \Gamma^{(v)} \frac{\Gamma_{xy}^{(s)}}{[1 - \Gamma_{xx}^{(s)}]^2 + [\Gamma_{xy}^{(s)}]^2} \quad (10)$$

where $\Gamma_{xx}^{(s)}$ ($\Gamma_{xy}^{(s)}$) is the diagonal (off-diagonal) component of the spin-vertex function, and $\Gamma^{(v)}$ is the velocity-vertex function, which are defined from the following equations: $n_c u_i^2 \sum_{\mathbf{k}} G_{\mathbf{k},0,v}^r v_x G_{\mathbf{k},0,v}^a = v \Gamma_{xx}^{(v)} \sigma^x + \Gamma_{xy}^{(v)} \sigma^y$ and $\sum_{\mathbf{k}} G_{\mathbf{k},0,v}^r v^j G_{\mathbf{k},0,v}^a = \Gamma^{(v)} \epsilon_{j\ell z} \sigma^\ell \alpha_R \nu_e / (2\hbar)$.

We numerically calculate the vertex functions ($\Gamma^{(v)}$, $\Gamma_{xx}^{(s)}$, and $\Gamma_{xy}^{(s)}$) and obtain the Rashba SOC (α_R) and Ising SOC (β_I) dependence of \mathcal{C}_\perp and \mathcal{C}_\parallel as shown in Fig. 3(a) and 3(b), respectively. Here, we choose $\mu = 0.1$ eV and $\Sigma_0 = 3$ meV (which corresponds to the relaxation time $\tau = 0.1$ ps). In the absence of Ising SOC, $\beta_I = 0$, we can demonstrate $\mathcal{C}_\perp \approx \mathcal{C}_\perp^0 \equiv \alpha_R / (2\Sigma_0)$ and $\mathcal{C}_\parallel = 0$. In the presence of the Ising SOC, it is found that \mathcal{C}_\perp is suppressed by the Ising SOC. We find that in \mathcal{C}_\parallel has a maximum as a function of α_R , at which \mathcal{C}_\parallel becomes comparable to \mathcal{C}_\perp . With the further increase in α_R , \mathcal{C}_\perp dominates the Edelstein effect. It is also noticed that the self-energy (Σ_0) dependence of \mathcal{C}_\perp and \mathcal{C}_\parallel are different from each other: \mathcal{C}_\perp is proportional to $1/\Sigma_0$, whereas \mathcal{C}_\parallel is independent of Σ_0 . Namely, unlike the conventional Edelstein effect (\mathcal{C}_\perp is dissipation quantity), \mathcal{C}_\parallel is dissipationless.

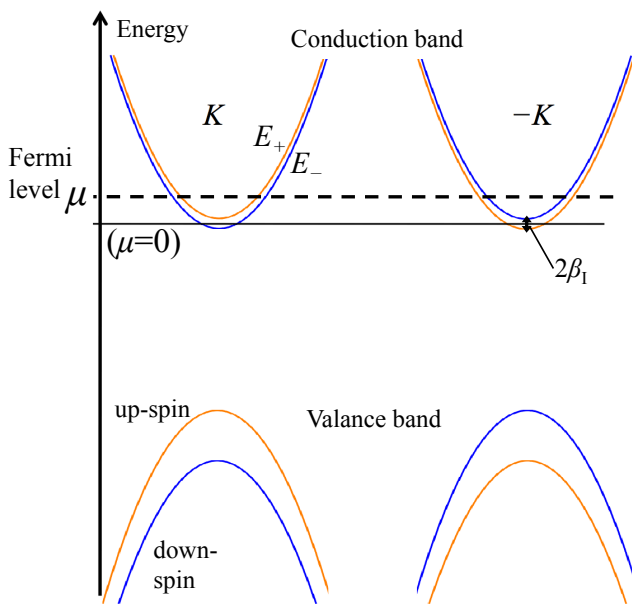


FIG. 2. (Color online) Spin-split conduction bands of the MTMD with the Ising SOC and Rashba SOC around K -point and $-K$ -point for $\mu > \beta_I$.

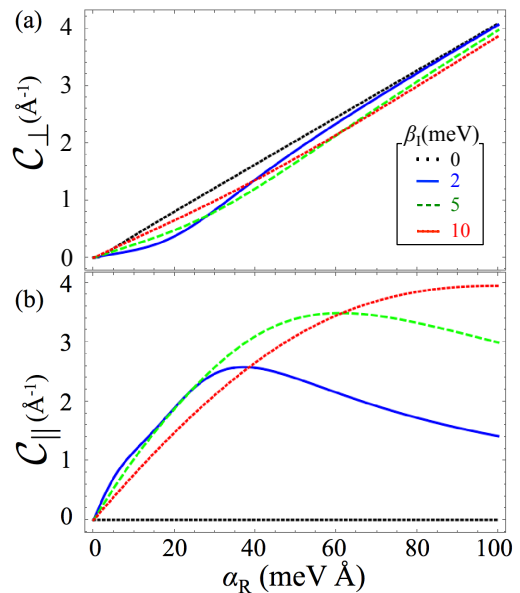


FIG. 3. (Color online) (a) Conventional and (b) valley-dependent part of the VEE as a function of the Rashba SOC (α_R) for various values of the Ising SOC (β_I) at bare self-energy $\Sigma_0 = 3$ meV and chemical potential $\mu = 0.1$ eV.

From analogy with the conventional Edelstein effect, we can explain why the VEE is generated by the Rashba and Ising SOC. In the absence of the Ising SOC, the conventional Edelstein effect is caused by the shift of the Fermi surface due to an applied electric field, as shown in Fig. 4 (a). In the absence of an external electric field, the total spin polarization on the Fermi surface is canceled out by integrating in the momentum space. An applied electric field \mathbf{E} shifts the Fermi surface and violates the spin balance on it, and hence, the net spin polarization survives, that corresponds to the first term of Eq. (1). In addition to this, in the presence of the Ising SOC, which is regarded as magnetization of each valleys, the applied electric field \mathbf{E} also triggers the valley-dependent Hall current due to the anomalous Hall effect [22, 40], and its current plays a role to shift the Fermi surface perpendicular to \mathbf{E} . As a result, the applied electric field shifts the Fermi surface not only along \mathbf{E} but also perpendicular to \mathbf{E} , as shown in Fig. 4 (b). Thus, the second term of Eq. (1) is caused by the Fermi surface shift via the Hall current. It is also noticed that since the direction of the Hall current depends on the sign of the Ising SOC, the shift of the Fermi surface and hence the second term of Eq. (1) depends on valley.

Experimental realization.— In this section, we point out that the strong SOC in MTMD materials allow us to readily observe the proposed Edelstein effects. The conventional Edelstein effect in Rashba SOC system has been reported in heterojunctions of InGaAs/InAlAs [41–45]. The α_R in this system is about 70 meV [41]. In the

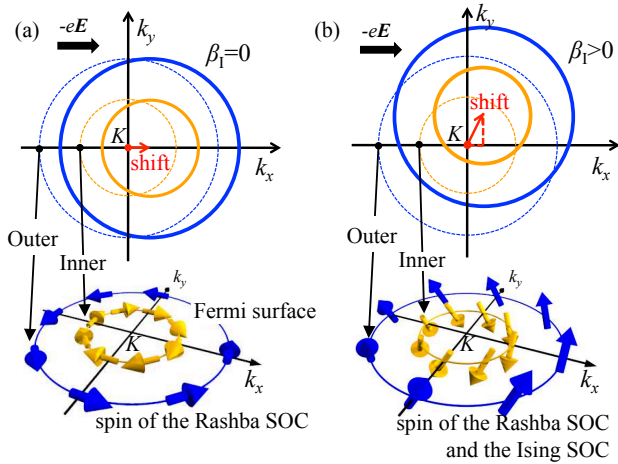


FIG. 4. (Color online) Mechanism for (a) the conventional Edelstein effect at $\beta_I = 0$ and (b) the VEE at $\beta_I \neq 0$. The top panels show the shift of the Fermi surface around the K point, where the dashed (solid) lines represent the spin-split Fermi surfaces in the absence (presence) of an applied electric field. The spin structures on the Fermi surface are depicted in the bottom panels. Due to the Ising SOC, the spins have the longitudinal component, which shifts the Fermi surfaces perpendicular to the applied field via the valley Hall effect as shown in (b).

setup of Fig. 1 (b), the α_R can easily exceed 70 meV using Tungsten based MTMD materials. For example, such a setup has been reported in an electric double-layer transistor based on WSe_2 single-crystal flakes under an external electric field [11]. In WSe_2 , the β_I in the conduction band near the K points is about 10 meV. Using these realistic parameters of the Ising and Rashba SOC, we find that in Fig. 3, there are parameter regimes in which C_{\parallel} is comparable to C_{\perp} . In the case of MoS_2 , the Ising SOC is about 5 meV in the conduction band of the K valleys as shown experimentally [16]. In this case, the VEE is still comparable to the conventional Edelstein effect as shown in Fig. 3.

The conventional Edelstein effect has been experimentally observed by using the Faraday effect [29] and the photoluminescence of polarized light [30]. These experimental methods can be used directly to detect the total spin polarization perpendicular to \mathbf{E} due to the conventional Edelstein effects in MTMD. The net spin polarization is $\langle \mathbf{s}_+ \rangle + \langle \mathbf{s}_- \rangle = 2e\nu_e C_{\perp} (\hat{z} \times \mathbf{E})$. For detection of the valley-dependent term in VEE, we can use circularly polarized light to excite electrons in a selected valley as in valley Hall effect measurements as illustrated in Fig. 5. In this case, the Fermi level is gated to be inside the band gap. When one can shine the circularly polarized light, the excited electrons from a particular valley will carry an induced spin polarization parallel to \mathbf{E} , which is approximately $e\nu'_e C_{\parallel} \mathbf{E}$. Similarly, the spin polarization perpendicular to \mathbf{E} is $e\nu'_e C_{\perp} (\hat{z} \times \mathbf{E})$. Here, ν'_e is the num-

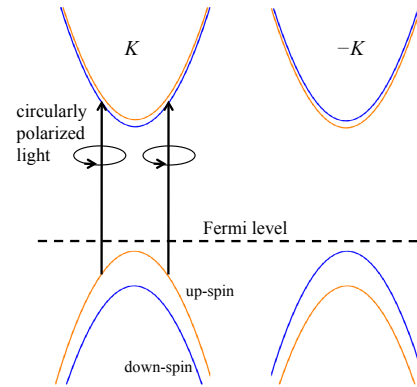


FIG. 5. (Color online) Schematic for valley-dependent electron excitation by a circularly polarized light, where the Fermi level is tuned in the band gap. The circularly polarized light selectively excites electrons in one of the valleys, making possible to detect valley dependent effects.

ber of electrons excited to the conduction band optically. Therefore, by controlling the Rashba coefficients through gating, we can manipulate the spin polarization direction as shown in Fig. 3.

Conclusion– In this work, we point out that, due to the Ising SOC and the valley Hall effect, the spin polarization of the current caused by an applied electric field has a component parallel to the electric field. The sign of this spin polarization is opposite at opposite valley. We call this effect the valley Edelstein effect. This valley Edelstein effect allows one to further control the spin polarization direction of the current in MTMD using electric fields. Importantly, this effect is very general and can appear in a large number of transition metal dichalcogenides such as in MoS_2 , WSe_2 and NbSe_2 which have different strength of spin-orbit couplings. It can also apply to other materials which break both the in-plane and out-of-plane mirror symmetries such as silicene in which both Ising SOC and Rashba SOC are present [46]. We believe our results are important for the electric field manipulation of the spin currents.

We acknowledge useful discussions with T. Yokoyama, T. Takenobu, and C.-Z. Chen. This work was supported by a Grant-in-Aid for the Core Research for Evolutional Science and Technology (CREST) of the Japan Science and Technology Corporation (JST) [JP-MJCR14F1] and by JSPS KAKENHI Grant Numbers JP15K17726, JP16H00989; K.T. is supported by a Grant-in-Aid for JSPS Fellows (Grants No. 13J03141). K. T. L thanks the support of HKRGC and Croucher Foundations through HKUST3/CRF/13G, C6026-16W, 16324216 and Croucher Innovation Grants.

-
- [1] X. Xu, W. Yao, D. Xiao, and T. F. Heinz, *Nat Phys* **10**, 343 (2014).
- [2] A. Splendiani, L. Sun, Y. Zhang, T. Li, J. Kim, C. Y. Chim, G. Galli, and F. Wang, *Nano Lett.* **10**, 1271 (2010).
- [3] K. F. Mak, C. Lee, J. Hone, J. Shan, and T. F. Heinz, *Phys. Rev. Lett.* **105**, 136805 (2010).
- [4] Q. H. Wang, K. Kalantar-Zadeh, A. Kis, J. N. Coleman, and M. S. Strano, *Nat. Nanotechnol.* **7**, 699 (2012).
- [5] A. K. Geim and I. V. Grigorieva, *Nature* **499**, 419 (2013).
- [6] A. Kuc, N. Zibouche, and T. Heine, *Phys. Rev. B*, **83**, 245213 (2011).
- [7] Z. Y. Zhu, Y. C. Cheng, and U. Schwingenschlöggl, *Phys. Rev. B* **84**, 153402 (2011).
- [8] F. Zahid, L. Liu, Y. Zhu, J. Wang, and H. Guo, *AIP Adv.* **3**, 52111 (2013).
- [9] H. Shi, H. Pan, Y.-W. Zhang, and B. I. Yakobson, *Phys. Rev. B* **87**, 155304 (2013).
- [10] E. Cappelluti, R. Roldán, J. A. Silva-Guillén, P. Ordejón, and F. Guinea, *Phys. Rev. B*, **88**, 075409 (2013).
- [11] H. Yuan, M. S. Bahramy, K. Morimoto, S. Wu, K. Nomura, B.-J. Yang, H. Shimotani, R. Suzuki, M. Toh, C. Kloc, X. Xu, R. Arita, N. Nagaosa, and Y. Iwasa, *Nat. Phys.* **9**, 563 (2013).
- [12] H. Rostami, A. G. Moghaddam, and R. Asgari, *Phys. Rev. B* **88**, 085440 (2013).
- [13] A. Kormányos, V. Zólyomi, N. D. Drummond, P. Rakyta, G. Burkard, and V. I. Falko, *Phys. Rev. B* **88**, 045416 (2013).
- [14] G.-B. Liu, W.-Y. Shan, Y. Yao, W. Yao, and D. Xiao, *Phys. Rev. B* **88**, 085433 (2013).
- [15] H. Ochoa and R. Roldán, *Phys. Rev. B* **87**, 245421 (2013).
- [16] J. M. Lu, O. Zheliuk, I. Leermakers, N. F. Q. Yuan, U. Zeitler, K. T. Law, and J. T. Ye, *Science* **350**, 1353 (2015).
- [17] X. Xi, Z. Wang, W. Zhao, J.-H. Park, K. T. Law, H. Berger, L. Forró, J. Shan, and K. F. Mak, *Nat. Phys.* **12**, 139 (2016).
- [18] F. Rose, M. O. Goerbig, and F. Piechon, *Phys. Rev. B* **88**, 125438 (2013).
- [19] Z. Song, R. Quhe, S. Liu, Y. Li, J. Feng, Y. Yang, J. Lu, and J. Yang, *Sci. Rep.* **5**, 13906 (2015).
- [20] D. Xiao, G. Bin Liu, W. Feng, X. Xu, and W. Yao, *Phys. Rev. Lett.* **108**, 196802 (2012).
- [21] T. Cao, G. Wang, W. Han, H. Ye, C. Zhu, J. Shi, Q. Niu, P. Tan, E. Wang, B. Liu, and J. Feng, *Nat. Commun.* **3**, 887 (2012).
- [22] K. F. Mak, K. L. McGill, J. Park, and P. L. McEuen, *Science* **344**, 1489 (2014).
- [23] A. G. Aronov and Y. B. Lyanda-Geller, *JETP Lett.* **52**, 431 (1989).
- [24] V. M. Edelstein, *Solid State Commun.* **73**, 233 (1990).
- [25] A. V. Chaplik, M. V. Entin, and L. I. Magarill, *Phys. E* **13**, 744, (2002).
- [26] J. Inoue, G. E. W. Bauer, and L. W. Molenkamp, *Phys. Rev. B* **67**, 033104, (2002).
- [27] K. Shen, G. Vignale, and R. Raimondi, *Phys. Rev. Lett.* **112**, 96601 (2014).
- [28] T. Yoda, T. Yokoyama, and S. Murakami, *Sci. Rep.* **5**, 12024 (2015).
- [29] Y. K. Kato, R. C. Myers, A. C. Gossard, and D. D. Awschalom, *Phys. Rev. Lett.* **93**, 176601 (2004).
- [30] A. Y. Silov, P. A. Blajnov, J. H. Wolter, R. Hey, K. H. Ploog, and N. S. Averkiev, *AIP Conf. Proc.* **772**, 1405 (2005).
- [31] M. Isasa, M. C. Martínez-Velarte, E. Villamor, C. Magén, L. Morellón, J. M. De Teresa, M. R. Ibarra, G. Vignale, E. V. Chulkov, E. E. Krasovskii, L. E. Hueso, and F. Casanova, *Phys. Rev. B* **93**, 14420 (2016).
- [32] J. Borge, C. Gorini, G. Vignale, and R. Raimondi, *Phys. Rev. B*, **89**, 245443 (2014).
- [33] H. Yuan, X. Wang, B. Lian, H. Zhang, X. Fang, B. Shen, G. Xu, Y. Xu, S.-C. Zhang, H. Y. Hwang, and Y. Cui, *Nat Nano* **9**, 851 (2014).
- [34] S. D. Ganichev and W. Prettl, *J. Phys. Condens. Matter* **15**, R935 (2003).
- [35] J. T. Ye, Y. J. Zhang, R. Akashi, M. S. Bahramy, R. Arita, and Y. Iwasa, *Science* **338**, 1193 (2012).
- [36] K. Taniguchi, A. Matsumoto, H. Shimotani, and H. Takagi, *Appl. Phys. Lett.* **101**, 42603 (2012).
- [37] N. F. Q. Yuan, K. F. Mak, and K. T. Law, *Phys. Rev. Lett.* **113**, 097001 (2014).
- [38] H. Haug and A. P. Jauho, *Quantum Kinetics in Transport and Optics of Semiconductors*, 2nd ed. (Springer, New York, 2007).
- [39] See the supplemental material for "Valley Edelstein Effect in Monolayer Transition Metal Dichalcogenides".
- [40] N. Nagaosa, J. Sinova, S. Onoda, A. H. MacDonald, and N. P. Ong, *Rev. Mod. Phys.* **82**, 1539 (2010).
- [41] J. Nitta, T. Akazaki, H. Takayanagi, and T. Enoki, *Phys. Rev. Lett.* **78**, 1335 (1997).
- [42] T. Koga, J. Nitta, H. Takayanagi, and S. Datta, *Phys. Rev. Lett.* **88**, 126601 (2002).
- [43] G. Lommer, F. Malcher, and U. Rossler, *Phys. Rev. Lett.* **60**, 728 (1988).
- [44] A. D. Caviglia, M. Gabay, S. Gariglio, N. Reyren, C. Cancellieri, and J. M. Triscone, *Phys. Rev. Lett.* **104**, 126803 (2010).
- [45] Y. Ohno, R. Terauchi, T. Adachi, F. Matsukura, and H. Ohno, *Phys. Rev. Lett.* **83**, 4196 (1999).
- [46] C.-C. Liu, H. Jiang, and Y. Yao, *Phys. Rev. B* **84**, 195430 (2011).
-

Supplemental Material for "Valley Edelstein Effect in Monolayer Transition Metal Dichalcogenides"

Katsuhisa Taguchi¹, Yuki Kawaguchi¹, Yukio Tanaka¹, and Kam Tuen Law²

¹*Department of Applied Physics, Nagoya University, Nagoya, 464-8603, Japan*

²*Department of Physics, Hong Kong University of Science and Technology, Clear Water Bay, Hong Kong, China*

We provide the calculation of \mathcal{C}_{\parallel} and \mathcal{C}_{\perp} for $\mu > \beta_{\text{I}}$ and $\mu < \beta_{\text{I}}$ [See Fig.S1]. Here, \mathcal{C}_{\parallel} and \mathcal{C}_{\perp} for $\mu > \beta_{\text{I}}$ are shown in Eq. (1) in the main text. Since preexisting works of the conventional Edelstein effect used Green's function techniques[1, 2], we also use Green's functions in the following calculation. The calculation is assumed when the magnitude of the self-energy of nonmagnetic impurity scattering is smaller than that of the chemical potential ($\mu \gg |\Sigma_{\text{v}}|$). Here, Σ_{v} is the self-energy of the nonmagnetic impurity scattering and its property depends on the Fermi level, as shown in Table. I.

CALCULATION OF \mathcal{C}_{\parallel} AND \mathcal{C}_{\perp} FOR $\mu < \beta_{\text{I}}$

First, we introduce the impurity-averaged Green's functions. When $\Sigma_z \ll \beta_{\text{I}}$ is satisfied, we have $u \approx \sqrt{\alpha_{\text{R}}^2 k^2 + \beta_{\text{I}}^2} - i\gamma\Sigma_z$ with $\gamma \equiv \frac{\beta_{\text{I}}}{\sqrt{\alpha_{\text{R}}^2 k^2 + \beta_{\text{I}}^2}}$. Then, the Green's function is described by the following form:

$$G_{\mathbf{k},\omega,\text{v}}^{\text{r}} = \frac{\Omega_{+}^{\text{r}}}{\hbar\omega - E_{+} + i(\Sigma'_{0} + \gamma\Sigma_z)} + \frac{\Omega_{-}^{\text{r}}}{\hbar\omega - E_{-} + i(\Sigma'_{0} - \gamma\Sigma_z)}, \quad (\text{S1})$$

$$G_{\mathbf{k},\omega,\text{v}}^{\text{a}} = \frac{\Omega_{+}^{\text{a}}}{\hbar\omega - E_{+} - i(\Sigma'_{0} + \gamma\Sigma_z)} + \frac{\Omega_{-}^{\text{a}}}{\hbar\omega - E_{-} - i(\Sigma'_{0} - \gamma\Sigma_z)}, \quad (\text{S2})$$

with

$$\Omega_{\pm}^{\text{r}} = \frac{1}{2} \left[1 \pm \frac{\mathbf{u}^{\text{r}} \cdot \boldsymbol{\sigma}}{u_0^{\text{r}}} \right], \quad u_0^{\text{r}} \equiv \sqrt{\alpha_{\text{R}}^2 k^2 + \beta_{\text{I}}^2} - i\gamma\Sigma_z, \quad (\text{S3})$$

$$\Omega_{\pm}^{\text{a}} = \frac{1}{2} \left[1 \pm \frac{\mathbf{u}^{\text{a}} \cdot \boldsymbol{\sigma}}{u_0^{\text{a}}} \right], \quad u_0^{\text{a}} \equiv \sqrt{\alpha_{\text{R}}^2 k^2 + \beta_{\text{I}}^2} + i\gamma\Sigma_z. \quad (\text{S4})$$

$\mathbf{u}^{\text{r}} [= (\mathbf{u}^{\text{a}})^*]$ is defined in the main text. Here, E_{\pm} denotes the energy dispersion of the spin-splitting bands $E_{\pm} = \epsilon_k \pm \sqrt{\alpha_{\text{R}}^2 k^2 + \beta_{\text{I}}^2}$. It is noticed that the first (second) term of Eqs. (S1)-(S2) is the Green's function corresponding to the upper (lower) spin split conduction band. Since the top conduction band is far from the Fermi level, contributions from the first term of Eqs. (S1)-(S2) in Eq. (1) in the main text are negligibly small compared with that from the second term of Eqs. (S1)-(S2). Hence the first term of Eqs. (S1)-(S2) is ignored in the following calculation. Besides, below, we simply use the following representation $\Omega_{-} \equiv \Omega_{-}^{\text{r}}$, $\Omega_{-}^{\dagger} \equiv \Omega_{-}^{\text{a}}$, $\mathbf{u} \equiv \mathbf{u}^{\text{r}}$, and $\mathbf{u}^* \equiv \mathbf{u}^{\text{a}}$.

From Eq. (6) in the main text, the spin density of each valley due to the applied electric field is given by

$$\langle s_{\text{v}}^{\text{VEE},i} \rangle = -\frac{e\hbar}{4\pi} \sum_{\mathbf{k}} \sum_{j=x,y} \text{tr} [\sigma^i G_{\mathbf{k},\text{v}}^{\text{r}} \mathcal{S}_{\mathbf{k},0,\text{v}}^j G_{\mathbf{k},\text{v}}^{\text{a}}] E_j. \quad (\text{S5})$$

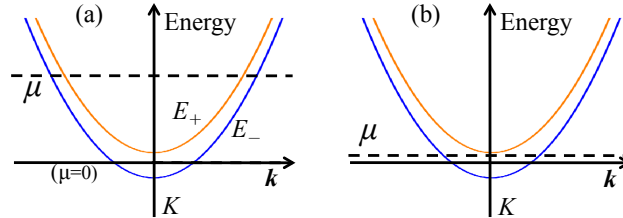


Figure S 1. Schematic illustration of spin-split conduction bands of the MTMD around K -point for (a) $\mu > \beta_{\text{I}}$ and (b) $-\beta_{\text{I}} \leq \mu \leq \beta_{\text{I}}$.

TABLE I. Self-energy due to the impurity scatterings in the presence of Rashba SOC and Ising SOC where $\Sigma'_{0,\omega=0}$ ($\Sigma_{z,\omega=0}$) is the spin and valley independent (dependent) part of the self-energy at $\omega = 0$, Σ_0 is the self-energy for a 2D metal, $u_R \equiv m\alpha_R^2/\hbar^2$, and $\lambda_0 = \beta_1^2 + u_R^2 - 2u_R\mu$. The dependence on the SOC strengths completely changes according to whether the Fermi level crosses one ($-\beta_1 \leq \mu \leq \beta_1$) or two ($\beta_1 < \mu$) conduction bands.

Fermi level	$\Sigma'_{0,\omega=0}/\Sigma_0$	$\Sigma_{z,\omega=0}/\Sigma_0$
$\mu > \beta_1$	1	0
$-\beta_1 \leq \mu \leq \beta_1$	$\frac{1}{2} + \frac{u_R}{2\sqrt{\lambda_0}}$	$\frac{\beta_1}{2\sqrt{\lambda_0}}$

\mathcal{S}_j is represented by

$$\mathcal{S}_{\mathbf{k},\omega,\mathbf{v}}^j = v_j + n_c u_1^2 \sum_{\mathbf{k}} G_{\mathbf{k},\omega,\mathbf{v}}^r v_j G_{\mathbf{k},\omega,\mathbf{v}}^a + (n_c u_1^2)^2 \sum_{\mathbf{k},\mathbf{k}_1} G_{\mathbf{k}_1,\omega,\mathbf{v}}^r G_{\mathbf{k},\omega,\mathbf{v}}^r v_j G_{\mathbf{k},\omega,\mathbf{v}}^a G_{\mathbf{k}_1,\omega,\mathbf{v}}^a + \dots, \quad (\text{S6})$$

where $v_j \equiv \partial\mathcal{H}_v/(\partial\hbar k_j)$ is the velocity operator. Here, $G_{\mathbf{k},v}^r [= (G_{\mathbf{k},v}^a)^\dagger]$ is defined by

$$G_{\mathbf{k},v}^r = \frac{\Omega_-}{-E_- + i(\Sigma'_0 - \gamma\Sigma_z)}. \quad (\text{S7})$$

Below, we use the following 2×2 matrix

$$\Gamma_j^{(s)} \equiv n_c u_1^2 \sum_{\mathbf{k}} G_{\mathbf{k},v}^r \sigma^j G_{\mathbf{k},v}^a = \sum_{\ell=x,y} \Gamma_{n\ell}^{(s)} \sigma^\ell. \quad (\text{S8})$$

$$\tilde{\Gamma}_j^{(v)} \equiv \sum_{\mathbf{k}} G_{\mathbf{k},v}^r v_j G_{\mathbf{k},v}^a = \sum_{n=x,y} \Gamma_{jn}^{(v)} \sigma^n. \quad (\text{S9})$$

Here, $\tilde{\Gamma}_j^{(s)}$ and $\Gamma_j^{(v)}$ denote the vertex function of the velocity operator and of the spin operator, respectively. $\tilde{\Gamma}_{jn}^{(s)}$ and $\Gamma_{jn}^{(v)}$ are coefficients of the matrix component of $\tilde{\Gamma}_j^{(s)}$ and $\Gamma_j^{(v)}$, respectively. Then, $\sum_{\mathbf{k}} G_{\mathbf{k},v}^r \mathcal{S}_{\mathbf{k},0,\mathbf{v}}^j G_{\mathbf{k},v}^a$ of Eq. (S47) is described by using $\Gamma_{jn}^{(v)}$ and $\Gamma_{jn}^{(s)}$ as

$$\begin{aligned} \sum_{\mathbf{k}} G_{\mathbf{k},v}^r \mathcal{S}_{\mathbf{k},0,\mathbf{v}}^j G_{\mathbf{k},v}^a &= \sum_{n=x,y} \tilde{\Gamma}_{jn}^{(v)} \left[\sigma^n + n_c u_1^2 \sum_{\mathbf{k}} G_{\mathbf{k},v}^r \sigma^n G_{\mathbf{k},v}^a + (n_c u_1^2)^2 \sum_{\mathbf{k},\mathbf{k}_1} G_{\mathbf{k}_1,v}^r G_{\mathbf{k},v}^r \sigma^n G_{\mathbf{k},v}^a G_{\mathbf{k}_1,v}^a + \dots \right] \\ &= \sum_{n,\ell=x,y} \tilde{\Gamma}_{jn}^{(v)} \left[\delta_{n\ell} + \Gamma_{n\ell}^{(s)} + \Gamma_{n\ell_1}^{(s)} \Gamma_{\ell_1\ell}^{(s)} + \dots \right] \sigma^\ell. \end{aligned} \quad (\text{S10})$$

As a result, Eq. (S5) is given by

$$\begin{aligned} \langle s_v^{\text{VEE},i} \rangle &= -\frac{e\hbar}{4\pi} \sum_{n,j,\ell=x,y} \tilde{\Gamma}_{jn}^{(v)} \left[\delta_{n\ell} + \Gamma_{n\ell}^{(s)} + \Gamma_{n\ell_1}^{(s)} \Gamma_{\ell_1\ell}^{(s)} + \dots \right] \text{tr} [\sigma^i \sigma^\ell] E_j \\ &= -\frac{e\hbar}{2\pi} \sum_{n,j=x,y} \tilde{\Gamma}_{jn}^{(v)} \left[\delta_{ni} + \Gamma_{ni}^{(s)} + \Gamma_{n\ell_1}^{(s)} \Gamma_{\ell_1 i}^{(s)} + \dots \right] E_j. \end{aligned} \quad (\text{S11})$$

Here, $\Gamma_{n\ell}^{(s)}$ and $\Gamma_{jn}^{(v)}$ are estimated by the following sections.

Calculation of Eq. (S8)

Equation (S8) is represented by

$$\Gamma_{n=x,y}^{(s)} = n_c u_1^2 \sum_{\mathbf{k}} G_{\mathbf{k},v}^r \sigma^{n=x,y} G_{\mathbf{k},v}^a = n_c u_1^2 \sum_{\mathbf{k}} \frac{\Omega_- \sigma^{n=x,y} \Omega_-^\dagger}{E_-^2 + (\Sigma'_0 - \gamma\Sigma_z)^2}. \quad (\text{S12})$$

Here, $\Omega_- \sigma^n \Omega_-^\dagger$ and the momentum-average of $\Omega_- \sigma^{n=x,y} \Omega_-^\dagger$ are given by

$$\Omega_- \sigma^n \Omega_-^\dagger = \left(\frac{1}{2} - \frac{u_a \sigma^a}{2u_0^r} \right) \sigma^n \left(\frac{1}{2} - \frac{u_b^* \sigma^b}{2u_0^a} \right) = \frac{1}{4} \sigma^n - \frac{u_a}{4u_0^r} \sigma^a \sigma^n - \frac{u_b^*}{4u_0^a} \sigma^n \sigma^a + \frac{u_a u_b^*}{4u_0^r u_0^a} \sigma^a \sigma^n \sigma^b, \quad (\text{S13})$$

$$\begin{aligned} \langle \Omega_- \sigma^{n=x,y} \Omega_-^\dagger \rangle_{\mathbf{k}} &= \frac{1}{4} \sigma^n + \frac{1}{4} \sum_{a,b=x,y,z} \frac{\langle u_a u_b^* \rangle_{\mathbf{k}}}{|u_0^r|^2} \sigma^a \sigma^n \sigma^b \\ &= \frac{1}{4} \sigma^n + \frac{\alpha_{\text{R}}^2 \epsilon_{apz} \epsilon_{bqz} \langle k_p k_q \rangle_{\mathbf{k}} + u_z u_z^* \delta_{az} \delta_{bz}}{4|u_0^r|^2} (\delta_{an} \sigma^b + \delta_{bn} \sigma^a - \delta_{ab} \sigma^n + i \epsilon_{abn}), \end{aligned} \quad (\text{S14})$$

where we have used $\langle u_a u_b^* \rangle_{\mathbf{k}} = \alpha_{\text{R}}^2 \epsilon_{apz} \epsilon_{bqz} \langle k_p k_q \rangle_{\mathbf{k}} + u_z u_z^* \delta_{az} \delta_{bz}$. Because of $\epsilon_{apz} \epsilon_{bqz} \langle k_p k_q \rangle_{\mathbf{k}} = 0$, Eq. (S14) is given by $\langle \Omega_- \sigma^{n=x,y} \Omega_-^\dagger \rangle_{\mathbf{k}} = \sigma^n (1 - u_z u_z^* / |u_0^r|^2) / 4$. Then, Eq. (S8) becomes

$$\Gamma_n^{(s)} = \frac{n_c u_1^2}{4} \sum_{\mathbf{k}} \frac{1}{E_-^2 + (\Sigma'_0 - \gamma \Sigma_z)^2} \left[1 - \frac{u_z u_z^*}{|u_0^r|^2} \right] \sigma^n. \quad (\text{S15})$$

From the above result, we have $\Gamma_{n\ell}^{(s)} = \Gamma^{(s)} \delta_{n\ell}$. $\Gamma^{(s)}$ is given by

$$\Gamma^{(s)} = \frac{\Sigma_0}{4\pi\nu_e} \sum_{\mathbf{k}} \frac{1}{E_-^2 + (\Sigma'_0 - \gamma \Sigma_z)^2} \left[1 - \frac{\beta_{\text{I}}^2 + \Sigma_z^2}{\alpha_{\text{R}}^2 k^2 + \beta_{\text{I}}^2 + \gamma^2 \Sigma_z^2} \right] = \frac{\Sigma_0}{4\pi} \int_0^\infty d\xi \frac{1}{E_\xi^2 + (\Sigma'_0 - \gamma \Sigma_z)^2} \left[1 - \frac{\beta_{\text{I}}^2 + \Sigma_z^2}{2u_{\text{R}}\xi + \beta_{\text{I}}^2 + \gamma^2 \Sigma_z^2} \right], \quad (\text{S16})$$

where we have used $\Sigma_0 = \pi\nu_e n_c u_1^2$, $u_{\text{R}} = m\alpha_{\text{R}}^2/\hbar^2$, and $E_\xi = \xi - \mu + \sqrt{2u_{\text{R}}\xi + \beta_{\text{I}}^2}$. Here, Σ_x , Σ_y , and γ are given by

$$\Sigma'_0 = \left[\frac{1}{2} + \frac{u_{\text{R}}}{2\sqrt{\lambda_0}} \right] \Sigma_0, \quad \Sigma_z = \frac{\beta_{\text{I}}}{2\sqrt{\lambda_0}} \Sigma_0, \quad \lambda_0 = \beta_{\text{I}}^2 - \mu^2 + (u_{\text{R}} - \mu)^2, \quad \gamma(\xi) = \frac{\beta_{\text{I}}}{\sqrt{2u_{\text{R}}\xi + \beta_{\text{I}}^2}}. \quad (\text{S17})$$

Calculation of Eq. (S9)

Equation (S9) is described by

$$\tilde{\Gamma}_j^{(v)} = \sum_{\mathbf{k}} \frac{\Omega_- v_j \Omega_-^\dagger}{E_-^2 + (\Sigma'_0 - \gamma \Sigma_z)^2}. \quad (\text{S18})$$

Here, $\Omega_- v_j \Omega_-^\dagger$ is estimated from $\mathbf{v} = +\hbar\mathbf{k}/m + \alpha_{\text{R}}(\mathbf{z} \times \boldsymbol{\sigma})/\hbar$ as

$$\begin{aligned} \Omega_- v_j \Omega_-^\dagger &= \left(\frac{1}{2} - \frac{u_n \sigma^n}{2u_0^r} \right) \left[+\frac{\hbar}{m} k_j + \frac{\alpha_{\text{R}}}{\hbar} \epsilon_{jzu} \sigma^u \right] \left(\frac{1}{2} - \frac{u_m^* \sigma^m}{2u_0^a} \right) \\ &= +\frac{\hbar}{m} k_j \left(\frac{1}{2} - \frac{u_n \sigma^n}{2u_0^r} \right) \left(\frac{1}{2} - \frac{u_m^* \sigma^m}{2u_0^a} \right) + \frac{\alpha_{\text{R}}}{\hbar} \epsilon_{jzu} \left(\frac{1}{2} - \frac{u_n \sigma^n}{2u_0^r} \right) \sigma^u \left(\frac{1}{2} - \frac{u_m^* \sigma^m}{2u_0^a} \right). \end{aligned} \quad (\text{S19})$$

The first term and the second term of the above equation are described by

$$(1) \equiv +\frac{\hbar}{m} k_j \left[\frac{1}{4} - \left(\frac{u_n}{4u_0^r} + \frac{u_n^*}{4u_0^a} \right) \sigma^n + \frac{u_n u_m^*}{4|u_0^r|^2} \sigma^n \sigma^m \right], \quad (\text{S20})$$

$$(2) \equiv \frac{\alpha_{\text{R}}}{\hbar} \epsilon_{jzu} \left[\frac{1}{4} \sigma^u - \frac{u_n}{4u_0^r} \sigma^n \sigma^u - \frac{u_m^*}{4u_0^a} \sigma^u \sigma^m + \frac{u_n u_m^*}{4|u_0^r|^2} \sigma^n \sigma^u \sigma^m \right]. \quad (\text{S21})$$

We will consider the following momentum-average $\langle \rangle_{\mathbf{k}}$:

$$\langle k_j \rangle_{\mathbf{k}} = 0, \quad (\text{S22})$$

$$\langle u_n \rangle_{\mathbf{k}} = u_z \delta_{nz}, \quad \langle u_m^* \rangle_{\mathbf{k}} = u_z^* \delta_{mz}, \quad (\text{S23})$$

$$\langle u_n u_m^* \rangle_{\mathbf{k}} = \alpha_{\text{R}}^2 \epsilon_{npz} \epsilon_{mqz} \langle k_p k_q \rangle_{\mathbf{k}} + u_z u_z^* \delta_{nz} \delta_{mz} \quad (\text{S24})$$

$$\langle k_j u_n \rangle_{\mathbf{k}} = \alpha_{\text{R}} \epsilon_{npj} \langle k_p k_j \rangle_{\mathbf{k}}, \quad \langle k_j u_m^* \rangle_{\mathbf{k}} = \alpha_{\text{R}} \epsilon_{mpz} \langle k_p k_j \rangle_{\mathbf{k}} \quad (\text{S25})$$

$$\langle k_j u_{v,n} u_{v,m}^* \rangle_{\mathbf{k}} = (\alpha_{\text{R}} \epsilon_{npj} \delta_{mz} u_z^* + \alpha_{\text{R}} \epsilon_{mpz} \delta_{nz} u_z) \langle k_p k_j \rangle_{\mathbf{k}}, \quad (\text{S26})$$

where we have used

$$\begin{aligned} u_n u_m^* &= (\alpha_R \epsilon_{npz} k_p + u_z \delta_{nz}) (\alpha_R \epsilon_{mqz} k_q + u_z^* \delta_{mz}) \\ &= \{ \alpha_R^2 \epsilon_{npz} \epsilon_{mqz} k_p k_q + u_z u_z^* \delta_{nz} \delta_{mz} \} + \{ \alpha_R \epsilon_{npz} \delta_{mz} u_z^* + \alpha_R \epsilon_{mpz} \delta_{nz} u_z \} k_p. \end{aligned} \quad (\text{S27})$$

Therefore, the first and second term are estimated by

$$\text{Eq. (S20)} = + \frac{\hbar \alpha_R}{4m} \langle k_p k_j \rangle_{\mathbf{k}} \left[- \left(\frac{1}{u_0^r} + \frac{1}{u_0^a} \right) \epsilon_{npz} \sigma^n + \frac{\epsilon_{npz} \delta_{mz} u_z^* + \epsilon_{mpz} \delta_{nz} u_z}{|u_0^r|^2} \sigma^n \sigma^m \right] \quad (\text{S28})$$

$$\text{Eq. (S21)} = \frac{\alpha_R}{4\hbar} \epsilon_{jzu} \left[\sigma^u - \frac{u_z}{u_0^r} \sigma^z \sigma^u - \frac{u_z^*}{u_0^a} \sigma^u \sigma^z + \frac{\alpha_R^2 \epsilon_{npz} \epsilon_{mqz} k_p k_q + u_z u_z^* \delta_{nz} \delta_{mz}}{|u_0^r|^2} \sigma^n \sigma^u \sigma^m \right]. \quad (\text{S29})$$

Then, $\langle \Omega_- v_j \Omega_-^\dagger \rangle_{\mathbf{k}}$ becomes

$$\begin{aligned} \langle \Omega_- v_j \Omega_-^\dagger \rangle_{\mathbf{k}} &= + \frac{\hbar \alpha_R}{4m} \langle k_p k_j \rangle_{\mathbf{k}} \left[- \frac{u_0^r + u_0^a}{|u_0^r|^2} \epsilon_{npz} \sigma^n + \frac{\epsilon_{npz} \delta_{mz} u_z^* + \epsilon_{mpz} \delta_{nz} u_z}{|u_0^r|^2} \sigma^n \sigma^m \right] \\ &\quad + \frac{\alpha_R}{4\hbar} \epsilon_{jzu} \left[\sigma^u - \frac{u_z}{u_0^r} \sigma^z \sigma^u - \frac{u_z^*}{u_0^a} \sigma^u \sigma^z + \frac{\alpha_R^2 \epsilon_{npz} \epsilon_{mqz} k_p k_q + u_z u_z^* \delta_{nz} \delta_{mz}}{|u_0^r|^2} \sigma^n \sigma^u \sigma^m \right]. \end{aligned} \quad (\text{S30})$$

From the above result, Eq. (S9) is described by

$$\begin{aligned} \tilde{\Gamma}_j^{(v)} &= \frac{\alpha_R}{4\hbar} \sum_{\mathbf{k}} \frac{1}{E_-^2 + (\Sigma'_0 - \gamma \Sigma_z)^2} \left\{ + \frac{\hbar^2 k^2}{2m} \left[- \frac{u_0^r + u_0^a}{|u_0^r|^2} \epsilon_{jzn} \sigma^n + \frac{\epsilon_{njz} \delta_{mz} u_z^* + \epsilon_{mjz} \delta_{nz} u_z}{|u_0^r|^2} \sigma^n \sigma^m \right] \right. \\ &\quad \left. + \epsilon_{jzu} \left[\sigma^u - \frac{u_z}{u_0^r} \sigma^z \sigma^u - \frac{u_z^*}{u_0^a} \sigma^u \sigma^z + \frac{\alpha_R^2 \epsilon_{npz} \epsilon_{mqz} k_p k_q + u_z u_z^* \delta_{nz} \delta_{mz}}{|u_0^r|^2} \sigma^n \sigma^u \sigma^m \right] \right\} \\ &= \frac{\alpha_R}{4\hbar} \sum_{\mathbf{k}} \frac{1}{E_-^2 + (\Sigma'_0 - \gamma \Sigma_z)^2} \left\{ \left(\frac{\hbar^2 k^2}{2m} \frac{u_0^r + u_0^a}{|u_0^r|^2} - 1 \right) \epsilon_{jaz} \sigma^a + \frac{\hbar^2 k^2}{2m} \frac{\epsilon_{njz} \delta_{mz} u_z^* + \epsilon_{mjz} \delta_{nz} u_z}{|u_0^r|^2} i \epsilon_{nml} \sigma^\ell \right. \\ &\quad \left. - \epsilon_{juz} \left[\left(- \frac{u_z}{u_0^r} + \frac{u_z^*}{u_0^a} \right) i \epsilon_{zua} \sigma^a + \frac{\frac{1}{2} \alpha_R^2 k^2 \delta_{nm} + u_z u_z^* \delta_{nz} \delta_{mz}}{|u_0^r|^2} \sigma^n \sigma^u \sigma^m \right] \right\} \\ &= \frac{\alpha_R}{4\hbar} \sum_{\mathbf{k}} \frac{1}{E_-^2 + (\Sigma'_0 - \gamma \Sigma_z)^2} \left\{ \left(\frac{\hbar^2 k^2}{2m} \frac{u_0^r + u_0^a}{|u_0^r|^2} - 1 \right) \epsilon_{jaz} \sigma^n + \frac{\hbar^2 k^2}{2m} \frac{\epsilon_{njz} \epsilon_{nza} u_z^* + \epsilon_{mjz} \epsilon_{zma} u_z}{|u_0^r|^2} i \sigma^a \right. \\ &\quad \left. - \epsilon_{juz} \left[\left(- \frac{u_z}{u_0^r} + \frac{u_z^*}{u_0^a} \right) i \epsilon_{zul} \sigma^\ell - \frac{u_z u_z^*}{|u_0^r|^2} \sigma^u \right] \right\} \\ &= \frac{\alpha_R}{4\hbar} \sum_{\mathbf{k}} \frac{1}{E_-^2 + (\Sigma'_0 - \gamma \Sigma_z)^2} \left\{ \left[\frac{\hbar^2 k^2}{2m} \frac{u_0^r + u_0^a}{|u_0^r|^2} - \left(1 - \frac{u_z u_z^*}{|u_0^r|^2} \right) \right] \epsilon_{jaz} \sigma^a + \left[- \frac{\hbar^2 k^2}{2m} \frac{u_z^* - u_z}{|u_0^r|^2} + \left(+ \frac{u_z^*}{u_0^a} - \frac{u_z}{u_0^r} \right) \right] i \sigma^j \right\} \end{aligned} \quad (\text{S31})$$

Here, we have used $\sum_{n,m=x,y} \sigma^m \sigma^u \sigma^m \delta_{nm} = 0$ and $\sigma^m \sigma^u \sigma^m \delta_{mz} \delta_{nz} = -\sigma^u$. Therefore, the above equation is given by

$$\begin{cases} \tilde{\Gamma}_{x,v}^{(v)} &= \tilde{\Gamma}_{xx,v}^{(v)} \sigma^x + \tilde{\Gamma}_{xy,v}^{(v)} \sigma^y \\ \tilde{\Gamma}_{y,v}^{(v)} &= \tilde{\Gamma}_{yx,v}^{(v)} \sigma^x + \tilde{\Gamma}_{yy,v}^{(v)} \sigma^y \end{cases} \quad (\text{S32})$$

with

$$\tilde{\Gamma}_{xy,v}^{(v)} = -\tilde{\Gamma}_{yx,v}^{(v)} = \frac{\alpha_R}{4\hbar} \sum_{\mathbf{k}} \frac{1}{E_-^2 + (\Sigma'_0 - \gamma \Sigma_z)^2} \left[\frac{\hbar^2 k^2}{2m} \frac{u_0^r + u_0^a}{|u_0^r|^2} - \left(1 - \frac{u_z u_z^*}{|u_0^r|^2} \right) \right]. \quad (\text{S33})$$

$$\tilde{\Gamma}_{xx,v}^{(v)} = \tilde{\Gamma}_{yy,v}^{(v)} = \frac{\alpha_R}{4\hbar} \sum_{\mathbf{k}} \frac{1}{E_-^2 + (\Sigma'_0 - \gamma \Sigma_z)^2} \left[- \frac{\hbar^2 k^2}{2m} \frac{u_z^* - u_z}{|u_0^r|^2} + \left(+ \frac{u_z^*}{u_0^a} - \frac{u_z}{u_0^r} \right) \right] i \quad (\text{S34})$$

Besides, we use $\mathbf{u} = \alpha_R(\mathbf{k} \times \mathbf{z}) + v(\beta_I - i\Sigma_z)\mathbf{z}$ and

$$u_0^r = \sqrt{\alpha_R^2 k^2 + (\beta_I - i\Sigma_z)^2} = \sqrt{\alpha_R^2 k^2 + \beta_I^2 - i\gamma\Sigma_z + o(\Sigma_z/\beta_I)}, \quad |u_0^r|^2 = \alpha_R^2 k^2 + \beta_I^2 + \gamma^2 \Sigma_z^2 + o(\Sigma_z/\beta_I), \quad (\text{S35})$$

$$\frac{u_z^* - u_z}{|u_0^r|^2} = v \frac{2i\Sigma_z}{\alpha_R^2 k^2 + \beta_I^2 + \gamma^2 \Sigma_z^2}, \quad \frac{u_z}{u_0^r} - \frac{u_z^*}{u_0^a} = -v 2i\Sigma_z \frac{\sqrt{\alpha_R^2 k^2 + \beta_I^2} - \gamma\beta_I}{\alpha_R^2 k^2 + \beta_I^2 + \gamma^2 \Sigma_z^2}, \quad (\text{S36})$$

$$\frac{u_0^r + u_0^a}{|u_0^r|^2} = \frac{2\sqrt{\alpha_R^2 k^2 + \beta_I^2}}{\alpha_R^2 k^2 + \beta_I^2 + \gamma^2 \Sigma_z^2}, \quad \frac{u_z u_z^*}{|u_0^r|^2} = \frac{\beta_I^2 + \Sigma_z^2}{\alpha_R^2 k^2 + \beta_I^2 + \gamma^2 \Sigma_z^2}. \quad (\text{S37})$$

Hence, using the above relations, $\tilde{\Gamma}_{xx}^{(v)}$ and $\tilde{\Gamma}_{xy}^{(v)}$ are represented by

$$\tilde{\Gamma}_{xy}^{(v)} = -\tilde{\Gamma}_{yx}^{(v)} = \frac{\alpha_R}{4\hbar} \sum_{\mathbf{k}} \frac{1}{E_+^2 + (\Sigma'_0 - \gamma\Sigma_z)^2} \left[\frac{\hbar^2 k^2}{m} \frac{\sqrt{\alpha_R^2 k^2 + \beta_I^2}}{\alpha_R^2 k^2 + \beta_I^2 + \gamma^2 \Sigma_z^2} - \left(1 - \frac{\beta_I^2 + \Sigma_z^2}{\alpha_R^2 k^2 + \beta_I^2 + \gamma^2 \Sigma_z^2} \right) \right], \quad (\text{S38})$$

$$\tilde{\Gamma}_{xx}^{(v)} = \tilde{\Gamma}_{yy}^{(v)} = +v \frac{\alpha_R}{2\hbar} \sum_{\mathbf{k}} \frac{\Sigma_z}{E_+^2 + (\Sigma'_0 - \gamma\Sigma_z)^2} \left[\frac{\hbar^2 k^2}{2m} - \frac{\sqrt{\alpha_R^2 k^2 + \beta_I^2} + \gamma\beta_I}{\alpha_R^2 k^2 + \beta_I^2 + \gamma^2 \Sigma_z^2} \right]. \quad (\text{S39})$$

It is noticed that from the result of $\Gamma^{(s)}$, $\tilde{\Gamma}_{xy}^{(v)}$ is also described by

$$\tilde{\Gamma}_{xy}^{(v)} = \frac{\alpha_R \nu_e}{2\hbar} \int_0^\infty d\xi \frac{1}{E_\xi^2 + (\Sigma'_0 - \gamma\Sigma_z)^2} \frac{\xi \sqrt{2u_R \xi + \beta_I^2}}{2u_R \xi + \beta_I^2 + \gamma^2 \Sigma_z^2} - \frac{\pi \nu_e \alpha_R}{\hbar \Sigma_0} \Gamma^{(s)} \quad (\text{S40})$$

with $E_\xi = +\xi - \mu + \sqrt{2u_R \xi + \beta_I^2}$. $\tilde{\Gamma}_{xx}^{(v)}$ is also described by

$$\tilde{\Gamma}_{xx}^{(v)} = +v \frac{\alpha_R \nu_e}{2\hbar} \int_0^\infty d\xi \frac{\Sigma_z}{E_\xi^2 + (\Sigma'_0 - \gamma\Sigma_z)^2} \left[\frac{\xi - \sqrt{2u_R \xi + \beta_I^2} + \gamma\beta_I}{2u_R \xi + \beta_I^2 + \gamma^2 \Sigma_z^2} \right]. \quad (\text{S41})$$

Result

Equation (S11) is estimated from Eqs. (S16), (S40), and (S41) as

$$\langle \mathbf{s}_v^{\text{VEE},x} \rangle = -\frac{e\hbar}{2\pi} [1 - \Gamma^{(s)}]^{-1} [\tilde{\Gamma}_{xx}^{(v)} E_x + \Gamma_{yx}^{(v)} E_y], \quad (\text{S42})$$

$$\langle \mathbf{s}_v^{\text{VEE},y} \rangle = -\frac{e\hbar}{2\pi} [1 - \Gamma^{(s)}]^{-1} [\tilde{\Gamma}_{xy}^{(v)} E_x + \tilde{\Gamma}_{yy}^{(v)} E_y]. \quad (\text{S43})$$

Because of $\tilde{\Gamma}_{xy}^{(v)} = -\tilde{\Gamma}_{yx}^{(v)}$ and $\tilde{\Gamma}_{xx}^{(v)} = \tilde{\Gamma}_{yy}^{(v)}$, the above equation is also represented by

$$\langle \mathbf{s}_v^{\text{VEE}} \rangle = -e\nu_e \mathcal{C}_\perp (\hat{\mathbf{z}} \times \mathbf{E}) - v e \nu_e \mathcal{C}_\parallel \mathbf{E}, \quad (\text{S44})$$

where \mathcal{C}_\perp and \mathcal{C}_\parallel are given by

$$\mathcal{C}_\perp = \frac{\hbar}{2\pi \nu_e} \left[\frac{\alpha_R \nu_e}{2\hbar} \int_0^\infty d\xi \frac{1}{E_\xi^2 + (\Sigma'_0 - \gamma\Sigma_z)^2} \frac{\xi \sqrt{2u_R \xi + \beta_I^2}}{2u_R \xi + \beta_I^2 + \gamma^2 \Sigma_z^2} - \frac{\alpha_R \nu_e}{2\hbar} \frac{2\pi}{\Sigma_0} \Gamma^{(s)} \right] [1 - \Gamma^{(s)}]^{-1} \equiv \frac{\alpha_R}{4\pi} \Gamma_{xy}^{(v)} [1 - \Gamma^{(s)}]^{-1},$$

$$\mathcal{C}_\parallel = \frac{\hbar}{2\pi \nu_e} \left(+ \frac{\alpha_R \nu_e}{2\hbar} \int_0^\infty d\xi \frac{\Sigma_z}{E_\xi^2 + (\Sigma'_0 - \gamma\Sigma_z)^2} \left[\frac{\xi - \sqrt{2u_R \xi + \beta_I^2} + \gamma\beta_I}{2u_R \xi + \beta_I^2 + \gamma^2 \Sigma_z^2} \right] \right) [1 - \Gamma^{(s)}]^{-1} \equiv + \frac{\alpha_R}{4\pi} \Gamma_{xx}^{(v)} [1 - \Gamma^{(s)}]^{-1},$$

with

$$\Gamma_{xy}^{(v)} \equiv \int_0^\infty \frac{1}{E_\xi^2 + (\Sigma'_0 - \gamma\Sigma_z)^2} \frac{\xi \sqrt{2u_R \xi + \beta_I^2}}{2u_R \xi + \beta_I^2 + \gamma^2 \Sigma_z^2} d\xi - \frac{2\pi}{\Sigma_0} \Gamma^{(s)}, \quad (\text{S45})$$

$$\Gamma_{xx}^{(v)} \equiv \int_0^\infty \frac{\Sigma_z}{E_\xi^2 + (\Sigma'_0 - \gamma\Sigma_z)^2} \frac{\xi - \sqrt{2u_R \xi + \beta_I^2} + \gamma\beta_I}{2u_R \xi + \beta_I^2 + \gamma^2 \Sigma_z^2} d\xi, \quad (\text{S46})$$

$$\Gamma^{(s)} = \frac{\Sigma_0}{4\pi} \int_0^\infty \frac{1}{E_\xi^2 + (\Sigma'_0 - \gamma\Sigma_z)^2} \left[1 - \frac{\beta_I^2 + \Sigma_z^2}{2u_R \xi + \beta_I^2 + \gamma^2 \Sigma_z^2} \right] d\xi.$$

Figure S 2 shows that the Ising SOC dependence of $\mathcal{C}_\parallel/\mathcal{C}_\perp$ in $\beta_I < \mu$ for several α_R . We find $\mathcal{C}_\parallel/\mathcal{C}_\perp < 1$ in the whole of β_I .

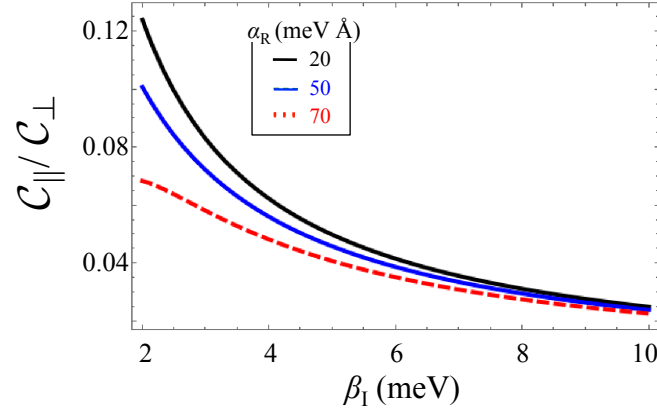


Figure S 2. The Ising SOC β_I dependence of C_{\parallel}/C_{\perp} in the conduction band in $\beta_I > \mu$ for several Rashba SOC (α_R) at $\Sigma_0 = 0.3$ meV.

CALCULATION OF C_{\parallel} AND C_{\perp} FOR $\mu > \beta_I$

Here, we provide the calculation C_{\parallel} and C_{\perp} for $\mu > \beta_I$. The results are shown in Eqs. (9)-(10) in the main text. Using the self-energy in Table I and Eq. (6) in the main text, we can represent $\langle s_v^{\text{VEE},i} \rangle$ as

$$\langle s_v^{\text{VEE},i} \rangle = -\frac{e\hbar}{4\pi} \sum_{\mathbf{k}} \text{tr}[\sigma^i G_{\mathbf{k},v}^r \mathcal{S}_j G_{\mathbf{k},v}^a] E_j. \quad (\text{S47})$$

Here, $\mathcal{S}_{\mathbf{k},\omega,v}^j$ is represented by

$$\mathcal{S}_{\mathbf{k},\omega,v}^j = v_j + n_c u_i^2 \sum_{\mathbf{k}} G_{\mathbf{k},\omega,v}^r v_j G_{\mathbf{k},\omega,v}^a + (n_c u_i^2)^2 \sum_{\mathbf{k},\mathbf{k}_1} G_{\mathbf{k}_1,\omega,v}^r G_{\mathbf{k},\omega,v}^r v_j G_{\mathbf{k},\omega,v}^a G_{\mathbf{k}_1,\omega,v}^a + \dots, \quad (\text{S48})$$

where the Green's functions in $\mu > \beta_I$ are given from Eqs. (S1) as

$$G_{\mathbf{k},v}^r \equiv \frac{\Omega_+}{-E_+ + i\Sigma_0} + \frac{\Omega_-}{-E_- + i\Sigma_0} \quad (\text{S49})$$

where we have used $E_{\pm} = \frac{\hbar^2 k^2}{2m} - \mu \pm u$ and $u = \sqrt{\alpha_R^2 k^2 + \beta_I^2}$.

To simply represent Eq. (S47), we introduce the following 2×2 matrix in $\mu > \beta_I$:

$$\Gamma_j^{(v)} \equiv \sum_{\mathbf{k}} G_{\mathbf{k},v}^r v_j G_{\mathbf{k},v}^a = \sum_{n=x,y} \Gamma_{jn}^{(v)} \sigma^n \quad (\text{S50})$$

$$\Gamma_j^{(s)} \equiv n_c u_i^2 \sum_{\mathbf{k}} G_{\mathbf{k},v}^r \sigma^j G_{\mathbf{k},v}^a = \sum_{\ell=x,y} \Gamma_{n\ell}^{(s)} \sigma^\ell. \quad (\text{S51})$$

Here, $\Gamma_{jn}^{(v)}$ and $\Gamma_{jn}^{(s)}$ are the matrix component of $\Gamma_j^{(v)}$ and $\Gamma_j^{(s)}$, respectively. Thus, the above 2×2 matrices are described by using Pauli matrices. Then, $\sum_{\mathbf{k}} G_{\mathbf{k},v}^r \mathcal{S}_j G_{\mathbf{k},v}^a$ of Eq. (S47) is described by

$$\begin{aligned} \sum_{\mathbf{k}} G_{\mathbf{k},v}^r \mathcal{S}_j G_{\mathbf{k},v}^a &= \sum_{n=x,y} \Gamma_{jn}^{(v)} \left[\sigma^n + n_c u_i^2 \sum_{\mathbf{k}} G_{\mathbf{k},v}^r \sigma^n G_{\mathbf{k},v}^a + (n_c u_i^2)^2 \sum_{\mathbf{k},\mathbf{k}_1} G_{\mathbf{k}_1,v}^r G_{\mathbf{k},v}^r \sigma^n G_{\mathbf{k},v}^a G_{\mathbf{k}_1,v}^a + \dots \right] \\ &= \sum_{n=x,y} [\Gamma^{(v)}]_{jn} \left[\delta_{n\ell} + \Gamma_{n\ell}^{(s)} + \Gamma_{n\ell_1}^{(s)} \Gamma_{\ell_1\ell}^{(s)} + \dots \right] \sigma^\ell \end{aligned} \quad (\text{S52})$$

Therefore, the spin density is given by

$$\begin{aligned} \langle s_v^i \rangle &= -\frac{e\hbar}{4\pi} \Gamma_{jn}^{(v)} \left[\delta_{n\ell} + \Gamma_{n\ell}^{(s)} + \Gamma_{n\ell_1}^{(s)} \Gamma_{\ell_1\ell}^{(s)} + \dots \right] \text{tr}[\sigma^i \sigma^\ell] E_j \\ &= -\frac{e\hbar}{2\pi} \Gamma_{jn}^{(v)} \left[\delta_{ni} + \Gamma_{ni}^{(s)} + \Gamma_{n\ell_1}^{(s)} \Gamma_{\ell_1 i}^{(s)} + \dots \right] E_j. \end{aligned} \quad (\text{S53})$$

$\Gamma_{n\ell}^{(s)}$ and $\Gamma_{jn}^{(v)}$ are estimated by Sec. and .

Calculation of $\Gamma_{nl}^{(s)}$ in $\mu > \beta_I$

To estimate $\Gamma_{nl}^{(s)}$, we calculate $\Gamma_n^{(s)}$. $\Gamma_j^{(s)}$ is represented by

$$\begin{aligned}\Gamma_{n=x,y}^{(s)} &= n_c u_i^2 \sum_{\mathbf{k}} G_{\mathbf{k},v}^r \sigma^n G_{\mathbf{k},v}^a \\ &= n_c u_i^2 \sum_{\mathbf{k}} \left[\frac{\Omega_+ \sigma^n \Omega_+}{E_+^2 + \Sigma_0^2} + \frac{\Omega_- \sigma^n \Omega_-}{E_-^2 + \Sigma_0^2} + \frac{\Omega_+ \sigma^n \Omega_-}{(E_+ - i\Sigma_0)(E_- + i\Sigma_0)} + \frac{\Omega_- \sigma^n \Omega_+}{(E_+ + i\Sigma_0)(E_- - i\Sigma_0)} \right].\end{aligned}\quad (\text{S54})$$

Here $\Omega_{\pm} \sigma^n \Omega_{\pm}$ and $\Omega_{\pm} \sigma^n \Omega_{\mp}$ are estimated by

$$\begin{cases} \Omega_{\pm} \sigma^{n=x,y} \Omega_{\pm} &= \pm \frac{u_n}{2u} + \frac{u_n u_a}{2u^2} \sigma^a \\ \Omega_- \sigma^n \Omega_+ &= \frac{1}{2} \sigma^n - i \frac{u_a}{u} \epsilon_{anl} \sigma^\ell - \frac{u_n u_a}{2u^2} \sigma^a \\ \Omega_+ \sigma^n \Omega_- &= \frac{1}{2} \sigma^n + i \frac{u_a}{u} \epsilon_{anl} \sigma^\ell - \frac{u_n u_a}{2u^2} \sigma^a \end{cases}.\quad (\text{S55})$$

The momentum average of the above equations become

$$\begin{cases} \langle \Omega_{\pm} \sigma^{n=x,y} \Omega_{\pm} \rangle_{\mathbf{k}} &= \frac{\alpha_R^2 k^2}{4u^2} \sigma^n \\ \langle \Omega_- \sigma^{n=x,y} \Omega_+ \rangle_{\mathbf{k}} &= \left(\frac{1}{2} - \frac{\alpha_R^2 k^2}{4u^2} \right) \sigma^n - i \frac{u_z}{u} \epsilon_{znl} \sigma^\ell, \\ \langle \Omega_+ \sigma^{n=x,y} \Omega_- \rangle_{\mathbf{k}} &= \left(\frac{1}{2} - \frac{\alpha_R^2 k^2}{4u^2} \right) \sigma^n + i \frac{u_z}{u} \epsilon_{znl} \sigma^\ell \end{cases},\quad (\text{S56})$$

where we have used $\langle u_a u_b \rangle_{\mathbf{k}} = \alpha_R^2 \epsilon_{apz} \epsilon_{bqz} \langle k_p k_q \rangle_{\mathbf{k}} + u_z u_z \delta_{az} \delta_{bz}$.

Therefore, we find that $\Gamma_{n=x,y}^{(s)}$ is described by the form $\Gamma_{n=x,y}^{(s)} = \Gamma_{n\gamma}^{(s)} \sigma^\gamma$:

$$\begin{aligned}\Gamma_{n\gamma}^{(s)} &= n_c u_i^2 \sum_{\mathbf{k}} \left[\frac{\alpha_R^2 k^2}{4u^2} \left(\frac{1}{E_+^2 + \Sigma_0^2} + \frac{1}{E_-^2 + \Sigma_0^2} - \frac{1}{(E_+ - i\Sigma_0)(E_- + i\Sigma_0)} - \frac{1}{(E_+ + i\Sigma_0)(E_- - i\Sigma_0)} \right) \right] \delta_{n\gamma} \\ &\quad + \frac{1}{2} n_c u_i^2 \sum_{\mathbf{k}} \left[\frac{1}{(E_+ - i\Sigma_0)(E_- + i\Sigma_0)} + \frac{1}{(E_+ + i\Sigma_0)(E_- - i\Sigma_0)} \right] \delta_{n\gamma} \\ &\quad + n_c u_i^2 \sum_{\mathbf{k}} \left[\frac{u_z}{u} \left(\frac{1}{(E_+ - i\Sigma_0)(E_- + i\Sigma_0)} - \frac{1}{(E_+ + i\Sigma_0)(E_- - i\Sigma_0)} \right) \right] i \epsilon_{zn\gamma}.\end{aligned}\quad (\text{S57})$$

As a result, we obtain

$$\begin{aligned}\Gamma_{xx}^{(s)} = \Gamma_{yy}^{(s)} &= n_c u_i^2 \sum_{\mathbf{k}} \left[\frac{\alpha_R^2 k^2}{4u^2} \left(\frac{1}{E_+^2 + \Sigma_0^2} + \frac{1}{E_-^2 + \Sigma_0^2} - \frac{1}{(E_+ - i\Sigma_0)(E_- + i\Sigma_0)} - \frac{1}{(E_+ + i\Sigma_0)(E_- - i\Sigma_0)} \right) \right] \\ &\quad + \frac{1}{2} n_c u_i^2 \sum_{\mathbf{k}} \left[\frac{1}{(E_+ - i\Sigma_0)(E_- + i\Sigma_0)} + \frac{1}{(E_+ + i\Sigma_0)(E_- - i\Sigma_0)} \right] \\ &= \frac{\Sigma_0}{\pi} \int_0^\infty d\xi \left[\frac{u_R \xi}{2u^2} \left(\frac{1}{E_+^2 + \Sigma_0^2} + \frac{1}{E_-^2 + \Sigma_0^2} - \frac{1}{(E_+ - i\Sigma_0)(E_- + i\Sigma_0)} - \frac{1}{(E_+ + i\Sigma_0)(E_- - i\Sigma_0)} \right) \right] \\ &\quad + \frac{\Sigma_0}{2\pi} \int_0^\infty d\xi \left[\frac{1}{(E_+ - i\Sigma_0)(E_- + i\Sigma_0)} + \frac{1}{(E_+ + i\Sigma_0)(E_- - i\Sigma_0)} \right] \\ &= \frac{\Sigma_0}{\pi} \int_0^\infty d\xi \frac{u_R \xi}{2u^2} \frac{(E_+ - E_-)^2}{(E_+^2 + \Sigma_0^2)(E_-^2 + \Sigma_0^2)} + \frac{\Sigma_0}{\pi} \int_0^\infty d\xi \frac{E_+ E_- + \Sigma_0^2}{(E_+^2 + \Sigma_0^2)(E_-^2 + \Sigma_0^2)} \\ &= \frac{\Sigma_0}{\pi} \int_0^\infty d\xi \frac{2u_R \xi + E_+ E_- + \Sigma_0^2}{(E_+^2 + \Sigma_0^2)(E_-^2 + \Sigma_0^2)} = \frac{\Sigma_0}{\pi} \int_0^\infty d\xi \frac{(\xi - \mu)^2 + \Sigma_0^2 - \beta_1^2}{(E_+^2 + \Sigma_0^2)(E_-^2 + \Sigma_0^2)},\end{aligned}\quad (\text{S58})$$

$$\begin{aligned}\Gamma_{xy}^{(s)} = -\Gamma_{yx}^{(s)} &= n_c u_i^2 \sum_{\mathbf{k}} \left[i \frac{u_z}{u} \left(\frac{1}{(E_+ - i\Sigma_0)(E_- + i\Sigma_0)} - \frac{1}{(E_+ + i\Sigma_0)(E_- - i\Sigma_0)} \right) \right] \\ &= \frac{\Sigma_0}{\pi} \int_0^\infty d\xi \left[i \frac{u_z}{u} \left[\frac{1}{(E_+ - i\Sigma_0)(E_- + i\Sigma_0)} - \frac{1}{(E_+ + i\Sigma_0)(E_- - i\Sigma_0)} \right] \right] = \frac{\Sigma_0}{\pi} \int_0^\infty d\xi \left[i \frac{u_z}{u} \frac{2i\Sigma_0(E_- - E_+)}{(E_+^2 + \Sigma_0^2)(E_-^2 + \Sigma_0^2)} \right] \\ &= \frac{\Sigma_0}{\pi} \int_0^\infty d\xi \left[\frac{u_z}{u} \frac{4u\Sigma_0}{(E_+^2 + \Sigma_0^2)(E_-^2 + \Sigma_0^2)} \right] = \frac{\Sigma_0}{\pi} \int_0^\infty d\xi \frac{4u_z \Sigma_0}{(E_+^2 + \Sigma_0^2)(E_-^2 + \Sigma_0^2)}\end{aligned}\quad (\text{S59})$$

where we have used $\Sigma_0 = \pi \nu_e n_c u_i^2$, $\alpha_R^2 k^2 = 2u_R \xi$, $u_R = m\alpha_R^2/\hbar^2$, $E_{\pm} = \xi - \mu \pm u$, and $u = \sqrt{2u_R \xi + \beta_1^2}$.

Calculation of $\Gamma_{xx}^{(v)}$ and $\Gamma_{xy}^{(v)}$ in $\mu > \beta_I$

To estimate $\Gamma_{jn}^{(v)}$, we calculate $\Gamma_j^{(v)}$. $\Gamma_j^{(v)}$ is represented by

$$\Gamma_{j,v}^{(v)} = \sum_{\mathbf{k}} \left[\frac{\Omega_+ v_j \Omega_+}{E_+^2 + \Sigma_0^2} + \frac{\Omega_- v_j \Omega_-}{E_-^2 + \Sigma_0^2} + \frac{\Omega_+ v_j \Omega_-}{(E_+ - i\Sigma_0)(E_- + i\Sigma_0)} + \frac{\Omega_- v_j \Omega_+}{(E_+ + i\Sigma_0)(E_- - i\Sigma_0)} \right]. \quad (\text{S60})$$

Here, the momentum average of $\Omega_+ \sigma^{n=x,y} \Omega_+$, $\Omega_- \sigma^n \Omega_-$, and $\Omega_{+,v} \sigma^n \Omega_{-,v}$, and $\Omega_- \sigma^n \Omega_+$ are estimated from

$$\langle \Omega_{\pm} v_j \Omega_{\pm} \rangle_{\mathbf{k}} = \frac{\alpha_R}{2\hbar u} \epsilon_{jz\ell} \sigma^{\ell} \left[\pm \frac{\hbar^2 k^2}{2m} + \frac{\alpha_R^2 k^2}{2u} \right] \quad (\text{S61})$$

$$\langle \Omega_{\pm} v_j \Omega_{\mp} \rangle_{\mathbf{k}} = \frac{\alpha_R}{\hbar} \epsilon_{jz\ell} \Omega_{\pm} \sigma^{j=x,y} \Omega_{\mp} = \frac{\alpha_R}{2\hbar u} \epsilon_{jz\ell} \sigma^{\ell} \left[\frac{\alpha_R^2 k^2}{2u} \right] \quad (\text{S62})$$

and we obtain

$$\Gamma_j^{(v)} = \Gamma_{j\ell}^{(v)} \sigma^{\ell}, \quad (\text{S63})$$

with

$$\Gamma_{j\ell}^{(v)} = -\frac{\alpha_R}{2\hbar} \epsilon_{j\ell z} \sum_{\mathbf{k}} \left[\frac{\alpha_R^2 k^2}{2u^2} \frac{(E_+ + E_-)^2 + 4\Sigma_0^2}{(E_+^2 + \Sigma_0^2)(E_-^2 + \Sigma_0^2)} + \frac{\hbar^2 k^2}{2mu} \frac{(E_- - E_+)(E_- + E_+)}{(E_+^2 + \Sigma_0^2)(E_-^2 + \Sigma_0^2)} \right].$$

We notice $\Gamma_{xy}^{(v)} = -\Gamma_{yx}^{(v)}$ and $\Gamma_{xx}^{(v)} = \Gamma_{yy}^{(v)} = 0$. The above equation is also represented by $\xi = \frac{\hbar^2 k^2}{2m}$ as

$$\Gamma_{j\ell}^{(v)} = -\frac{2\alpha_R \nu_e}{\hbar} \epsilon_{j\ell z} \int_0^{\infty} d\xi \frac{\frac{u_R}{u^2} [(\xi - \mu)^2 + \Sigma_0^2] - (+\xi - \mu)}{(E_+^2 + \Sigma_0^2)(E_-^2 + \Sigma_0^2)} \xi, \quad (\text{S64})$$

where we have used $E_{\pm} = \xi - \mu \pm u$, $E_+ + E_- = 2(\xi - \mu)$, $E_- - E_+ = -2u$, and $u = \sqrt{2u_R \xi + \beta_I^2}$.

Calculation of $\Gamma^{(v)}$ in Eqs. (9) and (10)

From Eqs. (S58), (S59), and (S69), Eq. (S53) is represented as

$$\langle s_v^{\text{VEE},i} \rangle = -e\nu_e C_{li} (\mathbf{E} \times \hat{\mathbf{z}})_{\ell} \quad (\text{S65})$$

with $C_{li} \equiv \Gamma^{(v)} [1 + \Gamma^{(s)} + (\Gamma^{(s)})^2 + \dots]_{li}$. Here, C_{li} is also described by $C_{li} = C_{xx} \delta_{li} + \epsilon_{liz} C_{xy}$. Hence, we find that the spin density is represented by Eq. (1) in the main text:

$$\begin{aligned} \langle \mathbf{s}_v^{\text{VEE}} \rangle &= e\nu_e [C_{xx} (\hat{\mathbf{z}} \times \mathbf{E}) - v C_{xy} \mathbf{E}], \\ &= e\nu_e [C_{\perp} (\hat{\mathbf{z}} \times \mathbf{E}) + v C_{\parallel} \mathbf{E}] \end{aligned} \quad (\text{S66})$$

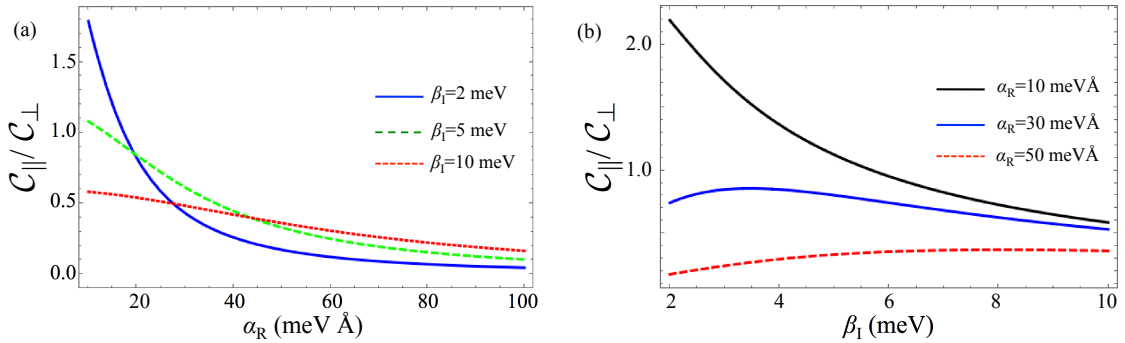


Figure S 3. (a) The Rashba SOC (α_R) dependence of C_{\parallel}/C_{\perp} for several the Ising SOC (β_I) in the conduction band in $\mu > \beta_I$. (b) β_I dependence of C_{\parallel}/C_{\perp} for several Rashba SOC (α_R). In these figures, we used $\Sigma_0 = 3$ meV and $\mu = 0.1$ eV. We find that C_{\parallel} can be comparable to C_{\perp} in a realistic parameter regime.

where the coefficients \mathcal{C}_\perp and \mathcal{C}_\parallel are given by

$$\mathcal{C}_\perp \equiv C_{xx} = \frac{\alpha_R}{4\pi} \Gamma^{(v)} \frac{1 - \Gamma_{xx}^{(s)}}{[1 - \Gamma_{xx}^{(s)}]^2 + [\Gamma_{xy}^{(s)}]^2} \quad (\text{S67})$$

$$\mathcal{C}_\parallel \equiv -C_{xy} = \frac{\alpha_R}{4\pi} \Gamma^{(v)} \frac{\Gamma_{xy}^{(s)}}{[1 - \Gamma_{xx}^{(s)}]^2 + [\Gamma_{xy}^{(s)}]^2} \quad (\text{S68})$$

Here, $\Gamma_{xx}^{(s)}$ and $\Gamma_{xy}^{(s)}$ are shown in Eq. (S58) and (S59), respectively. $\Gamma^{(v)}$ is defined

$$\Gamma^{(v)} = 4 \int_0^\infty d\xi \frac{\xi - \mu - \frac{u_R}{u^2} [(\xi - \mu)^2 + \Sigma_0^2]}{(E_+^2 + \Sigma_0^2)(E_-^2 + \Sigma_0^2)} \xi. \quad (\text{S69})$$

Figure S3(a) [(b)] shows the α_R [β_I] dependence of $\mathcal{C}_\parallel/\mathcal{C}_\perp$ for several β_I [α_R] in $\mu > \beta_I$. We find that \mathcal{C}_\parallel can be comparable to \mathcal{C}_\perp .



[1] V. M. Edelstein, Solid State Commun. **73**, 233 (1990).

[2] J. Inoue, G. E. W. Bauer, and L. W. Molenkamp, Phys. Rev. B **67**, 033104, (2002).